Nuclear Instruments and Methods in Physics Research A270 (1988) 140–145
North-Holland, Amsterdam

ON THE CALCULATION OF THE ENERGY LOSS OF MUONS IN SAMPLING CALORIMETERS

Bernd ANDERS *, Ulf BEHRENS and Hanno BRÜCKMANN

I. Institut für Experimentalphysik der Universität Hamburg, D-2000 Hamburg 50, FRG

Received 17 December 1987

A Monte Carlo (MC) technique has been used to investigate the energy loss of muons in sampling calorimetric devices. Two existing MC codes have been combined to calculate the muon transport with δ-electron-, bremsstrahlungs- and pair production (MUDEX) and the transport of these secondaries (EGS). The results show that with the help of such a detailed MC calculation, a precise calibration of sampling calorimeters is possible with muons.

1. Introduction

In discussing the performance of (high resolution) hadron sampling calorimeters [1], it is convenient to define sampling fractions R_i by

$$R_i := \frac{E_{\mathrm{vis},i}}{E_{\mathrm{invis},i} + E_{\mathrm{vis},i}} = \frac{E_{\mathrm{vis},i}}{E_{\mathrm{abs},i}}, \tag{1}$$

where the index i refers to different components in a hadronic shower, like $e^{\pm}$, $\mu^{\pm}$, $\pi^{\pm}$, π^0, η, K, p, n, etc., which deposit different fractions of their energy in the detector layers. $E_{\mathrm{vis},i}$ is the sum of the measured (mean) energy in all detector layers (fig. 1). $E_{\mathrm{invis},i}$ is the (mean) energy deposited in all absorber sheets. If the quantity $E_{\mathrm{abs}} = E_{\mathrm{invis}} + E_{\mathrm{vis}}$ is equal to the incident hadronic energy E_0, the calorimeter is called hermetic.

It is customary to normalize the sampling fractions to the sampling fraction R_{mip} for a minimum ionizing particle, mip [2]. Because muons have ionizing losses different from those of a mip, one has to distinguish between μ's and mip's. We abbreviate for an electromagnetic shower

$$\frac{\mathrm{e}}{\mathrm{mip}} := \frac{R_{\mathrm{e}}}{R_{\mathrm{mip}}}, \tag{2}$$

and for a muon:

$$\frac{\mu}{\mathrm{mip}} := \frac{R_{\mu}}{R_{\mathrm{mip}}}. \tag{3}$$

In the next section we explain the calculation of E_{vis} and E_{abs} for muons. We return to a discussion of the sampling fractions in the third section.

* DESY, Hamburg, FRG.

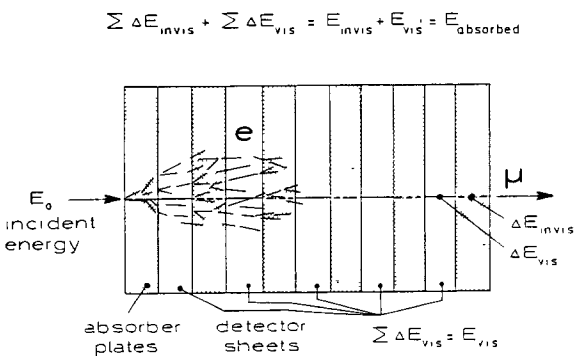

Fig. 1. Highly energetic electrons with incident energy E_0 induce an electromagnetic shower; muons dissipate a fraction of their energy between the absorber and detector layers. The energy "seen" by the detector material is called E_{vis}, the other part of the energy absorbed is called E_{invis}. The energy absorbed in the whole calorimeter stack E_{abs} might be (in the case of electrons) the whole incident energy E_0, but in the case of muons only a small part of E_0.

2. Calculation of the energy loss of muons

Since the fictitious mip's are not available for calibration, one frequently calibrates calorimeters with muons and calculates from the muon signal the signal for a mip. At low energies (several hundred MeV's) the muon behaves like a mip. At higher energies the relativistic rise becomes important and eventually bremsstrahlung, pair production and nuclear interactions become dominating. Fig. 2 illustrates the energy losses in bulk material of polystyrene and uranium [3].

Sandwich structures such as sampling calorimeters require a more sophisticated treatment than bulk material. This is illustrated in fig. 3, where the passage of a muon travelling through many interleaved layers of absorber (high Z) and detector (low Z) sheets is shown.

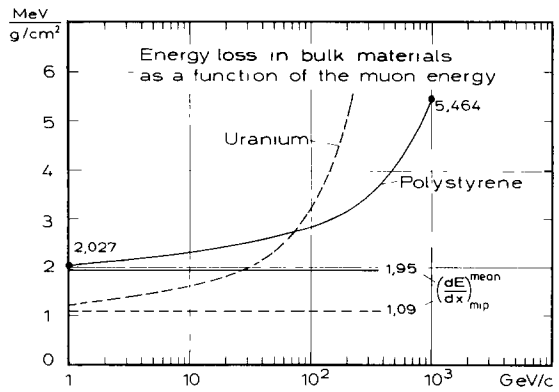

Fig. 2. The mean energy loss of muons in bulk material of polystyrene and uranium as a function of energy. The corresponding energy losses for minimum ionizing particles (mip's) are given for comparison [2].

The effects of δ-ray production, bremsstrahlung and e^+e^- pair production are energy- and material-dependent and are in general quite different for absorber and detector layers, and therefore E_{vis} and E_{invis} will have different energy dependences.

The quantity E_{vis} can best be calculated by a Monte Carlo procedure rather than by analytical means since δ-electrons created in the absorber can deposit part of their energy in the detector material and, vice versa, δ-electrons created in the detector can deposit part of their energy in the absorber material. Furthermore, bremsstrahlung and pair production give rise to electromagnetic showers, which can extend over several layers.

We use for the transport of the primary muon the Monte Carlo code MUDEX of Lohmann et al. [4]. This program produces randomly δ-electrons, bremsstrahlung gammas and electron/positron pairs according to the probabilities calculated by Bhabha [5], Petrukhin and Shestakov [6] as well as Kokoulin and Petrukhin [7]. Interactions with energy transfer below a given threshold are taken into account by calculating a mean value for this part of the energy loss. The energy is assumed to be deposited locally. In a second step, using EGS4 [9], each of the produced higher energetic δ-rays,

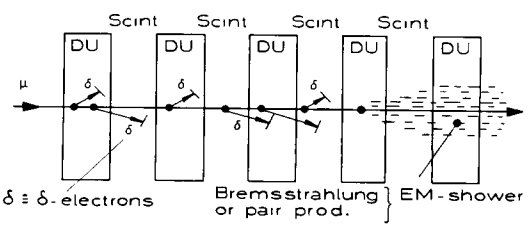

Fig. 3. When a muon is travelling through many interleaved layers of absorber and detector sheets, the effects of the production of δ-electrons, bremsstrahlung and e^+e^- pairs become increasingly important with higher energies.

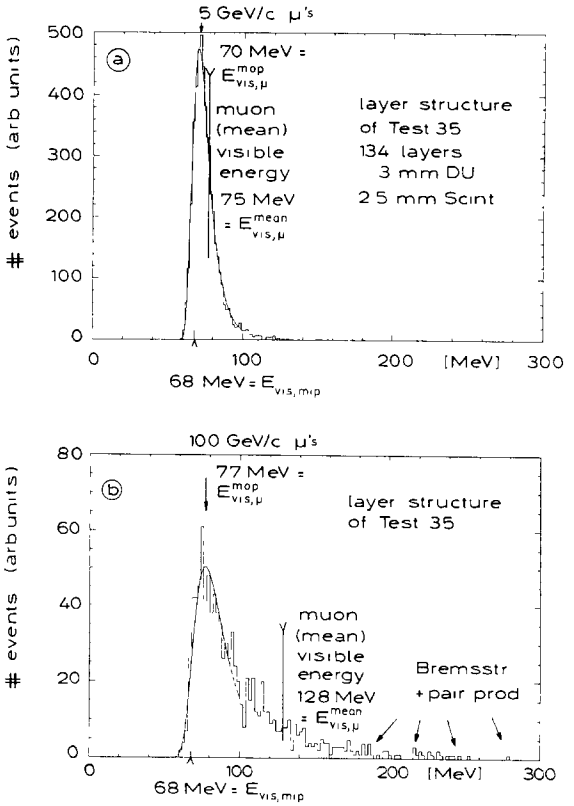

Fig. 4. The visible muon signal from MEGS calculations described in the text. (a) 5 GeV/c μ^- incident, 5000 events generated, CPU time ≈ 40 min. (b) 100 GeV/c μ^- incident, 1000 events generated, CPU time ≈ 40 min.

bremsstrahlung and particle pairs is followed through the calorimeter. We call the new code obtained by linking MUDEX to EGS4 the program MEGS [10].

The distributions of the visible energy as calculated with MEGS for 5 and 100 GeV muons are shown in figs. 4a and b for a uranium/scintillator test calorimeter (T35) with 134 layers of 3 mm thick depleted uranium (DU) plates and 2.5 mm thick scintillator (SCSN 38) plates [8]. As expected, the distributions of $E_{vis,\mu}$ exhibit a long tail extending to high energies. At 100 GeV (actually above 10 GeV) the calculated distributions deviate from a Landau distribution (dotted curve) due to the contributions from bremsstrahlung and pair production. The distributions have been fit to a 3-parameter Moyal function [13,14]. This function was introduced to describe Landau distributions in an analytical form. From these fits, the most probable value, mop, can be read off which is defined as the energy value where the maximum of the Moyal function occurs. The (mean) visible energy for a mip, $E_{vis,mip} = 68$ MeV, and for muons of 5 (100) GeV the most probable visible energy $E^{mop}_{vis,\mu} = 70$ (77) MeV and the mean visible energy $E^{mean}_{vis,\mu} = 75$ (128) MeV is also shown.

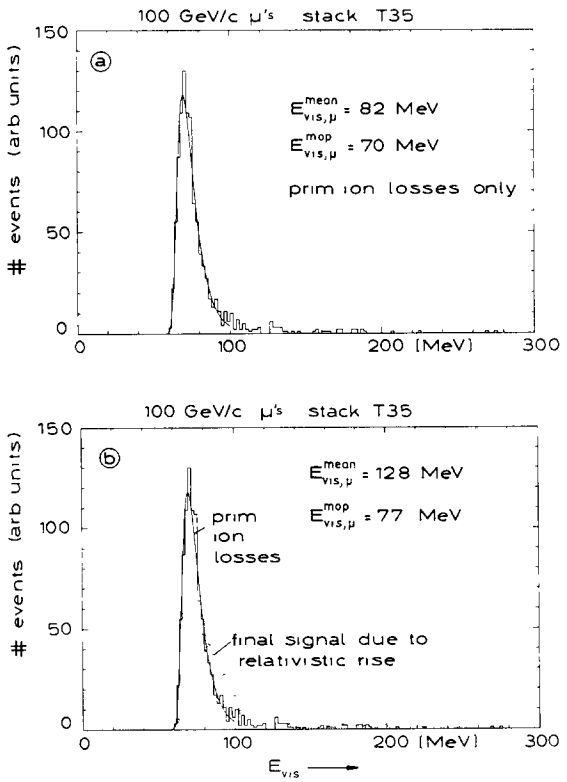

Fig. 5. (a) The visible muon signal from fig. 4b, if the only contributing processes would be the primary ionization due to the incident muon, showing the expected Landau distribution as a Moyal function fit (solid curve). (b) The solid curve is again the primary ionization from (a). When the secondary radiation (bremsstrahlung and e^+e^- pairs) is explicitly transported throughout the whole stack, the dissipated mean energy is increased. The result is shown by the dotted curves (histogram and Moyal fit, identical to fig. 4b).

The MC results can now be used to calibrate the experimental muon signal, which is obtained in arbitrary pulse height units. We propose to use as a starting point the most probable deposited energy, which in general can be determined more accurately from the data than the (mean) average energy loss.

Fig. 5a shows the MEGS result for the primary ionization losses which follows a Landau distribution. The solid curve shows the fit to a Moyal function up to 100 MeV. No transportation of (secondary) bremsstrahlung and e^+e^- pair production is included. In fig. 5b the sum of all these contributions is shown as dotted curve: The signal is the Moyal fit corresponding to fig. 4b as a smooth curve. The contributions from bremsstrahlung and pair production increase the mop-value from 70 MeV (fig. 5a) to 77 MeV (fig. 4b).

A similar but much stronger deviation from a Landau distribution is observed for the distribution of the absorbed energy $E_{abs,\mu} = E_{invis,\mu} + E_{vis,\mu}$ (fig. 6). The calculation gives $E^{mop}_{abs,\mu} = 1324$ MeV and $E^{mean}_{abs,\mu} = 2573$ MeV.

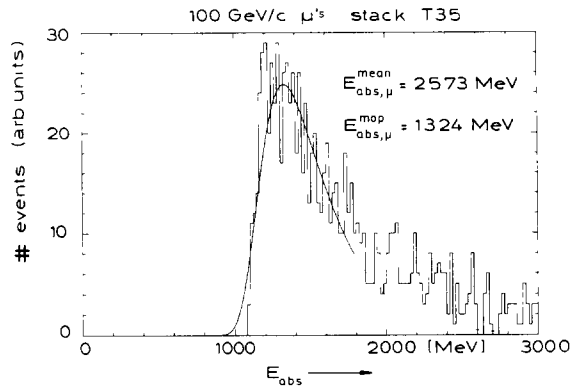

Fig. 6 The absorbed (invisible plus visible) muon signal for 100 GeV/c muons. There is a strong deviation from a pure Landau distribution (Moyal fit, solid and dotted curve) due to enhanced secondary radiation production in the high Z absorber layers.

The deposited energies in the scintillator, as calculated by MEGS, are compared in table 1 with the values given by ref. [3] for the mean energy loss in bulk scintillator material.

For 5 GeV/c the transport of δ-electrons out of the scintillator sheets (2.5 mm thickness) leads to a 8.5% reduction of visible energy for the scintillator layers as compared to the result of ref. [3]. We note that the MEGS value could depend somewhat on the energy cuts used in EGS4 and PEGS4 for the simulation of the low energy electron transport. A lowering of the cuts, due to the experience gained with related problems discussed in ref. [1], would decrease this reduction by a few percent.

For 100 GeV/c the modification of the signal is mainly due to bremsstrahlung and pair production, resulting in a 27% increase of the (mean) signal detected via the scintillator plates.

In the following we illustrate the usefulness of calibrating calorimeters via muons and the MEGS code. As an example, we show in fig. 7a the measured pulse height distribution from 5 GeV/c muons on T35 for a gate width of 100 ns. To account for the additional

Table 1
Deposited (mean) energy in the scintillator for 5 and 100 GeV/c muons incident on the T35 structure, as given by [3] and calculated by MEGS (lower row). The standard options for ECUT = AE = 1.5 MeV, PCUT = AP = 0.1 MeV and the step-size algorithm have been used in EGS4/PEGS4.

$E_0(\mu)$	5 GeV	100 GeV
$E^{scint}_{vis,\mu}$ for bulk material [3]	82 MeV	102 MeV
$E^{mean}_{vis,\mu}$ (MEGS)	75 MeV	128 MeV

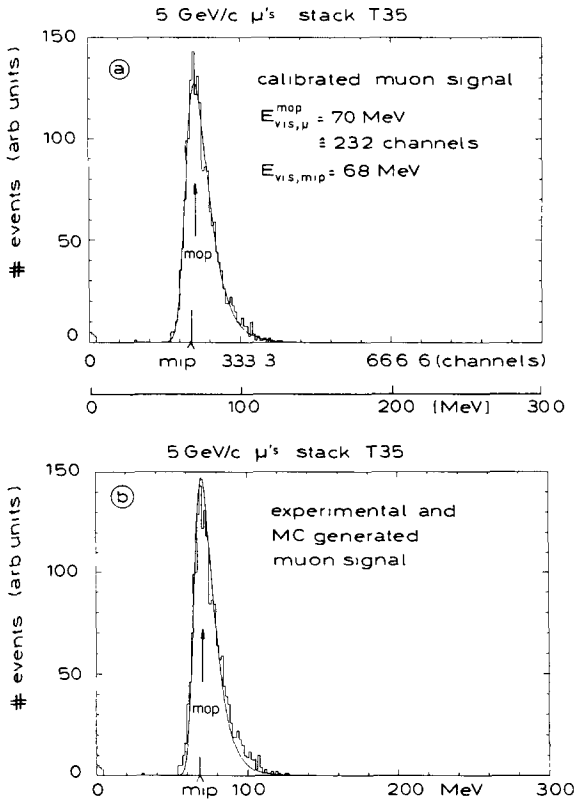

Fig. 7. (a) Calibrated muon signal from a test experiment (T35, [8]) at 5 GeV/c. The mean and mop values are taken from a MEGS calculation, see fig. 4a. The solid curve is a fit with a Moyal/Gaussian convolution to the data, resulting in a $E^{mop}_{vis,\mu}$ value given in channels. (b) The same experimental signal as in (a), but the solid curve is now a convolution of the Moyal function fitted to the corresponding MC generated (noise-free) muon distribution with a Gaussian fitted to the corresponding uranium noise distribution.

contributions from uranium noise and photostatistics, the fit function consisted of a convolution of a Gaussian with a Moyal function. Four parameters were fitted: the mop-value and the width of the Moyal function, the width of the Gaussian and an overall height factor. The solid curve in fig. 7a shows the result. The calibration factor is obtained by identifying the mop-value (in channels) with the mop-value from fig. 4a (in MeV). To check if the MEGS generated distribution can describe the experimental signal (the histogram shown in fig. 7a), we use now the parameters of the Moyal function (fig. 4a) to represent the experiment. This (noise-free) function is now convoluted with a Gaussian, which represents the uranium noise distribution see e.g. ref. [8], i.e. the width of the Gaussian is taken from the experimentally measured uranium noise signal. The result of this (parameter-free) convolution is shown in fig. 7b; it gives a good description of the experimental distribution.

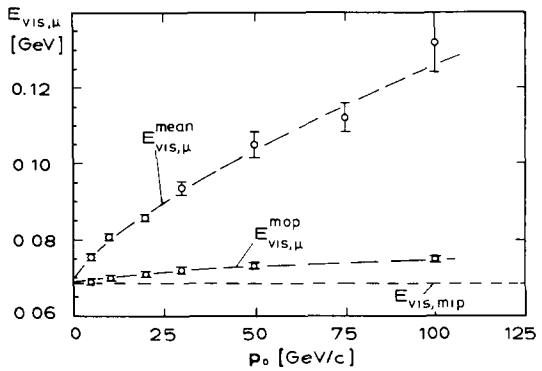

Fig. 8. The visible energy in a test calorimeter containing 134 scintillator–absorber layers [8] has been calculated by the MC program MEGS as a function of the muon energy. The mean and the most probable (mop) values are given. The latter is more convenient for calibrational purposes, because the long high energy tail of the μ spectrum mixes with hadronic events in an experimental test.

We conclude that the simulation of a muon signal distribution in sampling calorimeters can be performed in a realistic way using the MEGS code. Because of this the sampling fractions introduced in eq. (1) can now be expressed in terms of the muon parameters. Fig. 8 shows as a function of incident energy the behaviour of the visible mop and mean energies for muons.

3. Sampling fractions for electrons and muons

The physics of the sampling fraction of an electromagnetic shower has been discussed before. For high Z absorbers the sampling fraction for e or γ is considerably smaller than for mip's. This is due to the fact that a large fraction of the shower energy is carried by low energy ($E < 2$ MeV) photons (see refs. [11,15]), which are absorbed preferentially in the high Z absorber plates (migration effect of γ energy for sampling calorimeters [1,11,16]). We note that the normalized sampling fraction e/mip is a convenient (measurable) quantity to characterize a sampling device independent of the stack lenght L_0 and the incoming energy E_0. Although e/mip and μ/mip are defined in the same way (eqs. (2), (3)), there is a fundamental difference between the two quantities as illustrated by fig. 9. The difference arises because usual sampling calorimeters are always sufficient in depth to contain the whole electromagnetic shower ($E_0(\mathrm{e}) = E_{\mathrm{abs,e}}$), whereas in practice a calorimeter is a "thin target" for high energetic muons ($E_0(\mu) \gg E_{\mathrm{abs},\mu}$).

The normalized sampling fraction for muons, μ/mip, is therefore decreasing from 1 with increasing energy, whereas e/mip stays constant with E_0. It is clear from

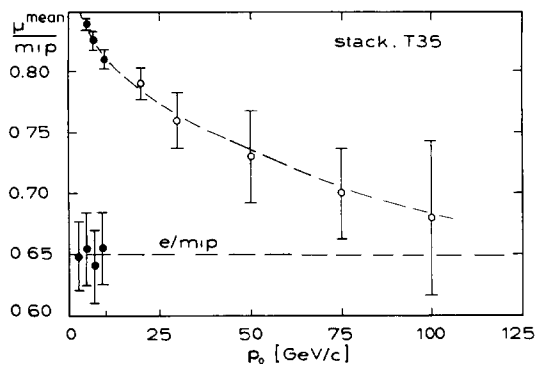

Fig. 9. The calculated normalized sampling fractions for muons (μ/mip ratio) and the e/mip ratios are shown as a function of incident energy E_0 for a uranium/scintillator calorimeter. The black dots correspond to experimentally determined numbers from T35 [8].

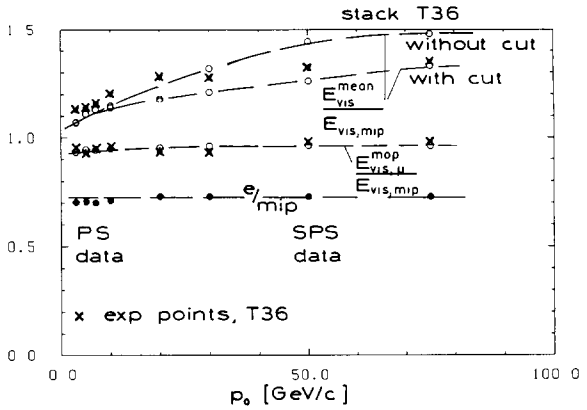

Fig. 10. Deposited energy ratios for the scintillator plates of a lead/scintillator test calorimeter, T36 [17]. Results from MEGS are denoted by open circles; the experimental results are shown as crosses.

such an energy dependence that the ratio μ/mip is not a practical quantity to characterize a sampling device.

This situation does not improve very much if one uses a different defined ratio to characterize the muon behaviour:

$$Q_\mu := E^{\mathrm{mop}}_{\mathrm{vis},\mu}/E^{\mathrm{mop}}_{\mathrm{abs},\mu}, \quad (4)$$

though $E^{\mathrm{mop}}_{\mathrm{vis},\mu}$ is not as energy dependent as $E^{\mathrm{mean}}_{\mathrm{vis},\mu}$ (see fig. 8). Especially the value for the denominator is not easily obtained (see fig. 6) for higher muon energies. To summarize, we state that instead of quoting e/μ ratios (which can only be meaningful for the specific calorimeter stack for which they are measured), one should give e/mip ratios, which can be obtained with the help of a calibration constant (see table 2).

Of course, if one is only interested in e/h ratios of a sampling device, one does not need such a calibration constant nor the e/mip intermediate result. But it is very helpful to do so, both for the experiments and the MC predictions (see refs. [1,16]), to make quoted results for e/h ratios more transparent and also more reliable.

Table 2
Various sampling fractions and ratios derived for the T35 calorimeter structure

$E_0(\mu)$	5 GeV	50 GeV	100 GeV
mip [a]	7.6%	7.6%	7.6%
e	4.94%	4.94%	4.94%
μ^{mean}	6.35%	5.46%	4.99%
μ^{mop}	6.49%	6.21%	5.82%
mip/μ^{mean} [b]	1.20	1.39	1.52
e/mip	0.65 ± 0.03	0.65	0.65
μ^{mean}/e	1.29	1.105	1.01
μ^{mop}/e	1.31	1.26	1.18

[a] The density of SCSN 38 has been measured to be $\rho = 1.044$ g/cm^3.

[b] In an earlier publication [12], published in Nucl. Instr. and Meth., the ratio "mip/μ" was preliminary used with a different meaning. Now the ratio used in ref. [12] would have to be written "mip/μ": $= E_{\mathrm{vis,mip}}/E^{\mathrm{scint}}_{\mathrm{vis},\mu}$. The values for $E^{\mathrm{scint}}_{\mathrm{vis},\mu}$ have been taken from the CERN table [3] for bulk material.

For the T35 sampling structure (3 mm DU, 2.5 mm scintillator), we gave as a first experimental result e/mip = 0.65 ± 0.03, using MEGS for calibration (see fig. 9). This result is in agreement with the value from the HELIOS collaboration, quoted earlier [16], as 0.67 ± 0.05 for the same layer structure. Unfortunately there are no high energy data for T35, but for a lead/scintillator sampling test calorimeter called T36 [17], equipped with 10 mm Pb and 2.5 mm SCSN 38. Their experimental results up to 75 GeV/c have been recalibrated with MEGS (ratio $E^{\mathrm{mop}}_{\mathrm{vis,mip}}/E_{\mathrm{vis,mip}}$; mip = 3.82%; see fig. 10). The ratios $E^{\mathrm{mean}}_{\mathrm{vis},\mu}/E_{\mathrm{vis,mip}}$ (called $\Delta\mu/\Delta$mip in ref. [17]) are also re-evaluated and are plotted in fig. 10. Since the experimental $E^{\mathrm{mean}}_{\mathrm{vis},\mu}$ values have been obtained by applying a high energy cut to the data, correspondingly we have used a cut at 50 MeV for the MEGS calculations. Nevertheless the E_0 dependence can only be poorly reproduced, probably due to difficulties in the evaluation of the experimental mean values mentioned earlier. So again the use of mop values should be the optimal option for comparison and evaluation of the e/mip values (see fig. 10). Our result for T36 is now 0.71 ± 0.03 (averaged over the PS and SPS data).

4. Summary

The Monte Carlo code MEGS has been developed for the description of the energy loss of muons in sampling calorimeters. The code has been obtained by combining the program MUDEX for the passage of the

primary muon with the program EGS to include the energy deposition by δ-electrons, bremsstrahlung and e^+e^- pairs. A quantitative description of the energy deposited by the muons is obtained. This offers the possibility to calibrate sampling calorimeters with the help of muons.

Acknowledgements

We are very much indebted to R. Voss from CERN/EP who provided us with the MUDEX Monte Carlo code and helped us with many hints to convert the code from the CERN version (written for a CDC computer) to the DESY IBM. Special thanks are given to E. Bernardi who provided us with the rediscovery of the Moyal function as a very useful tool to simulate the non-analytical Landau distribution. We deeply thank G. Wolf for many helpful comments on the manuscript. We are, as always, very much indebted to Mrs. M. Berghaus for carefully preparing all the drawings and typing the manuscript.

References

[1] H. Brückmann, B. Anders, U. Behrens, P. Cloth and D. Filges, Proc. 16th Winter Meeting on Fundamental Physics, Sevilla, Spain (1987) and DESY 87-064, Hamburg (1987).
[2] Review of Particle Properties, Phys. Lett. 170B (1986).
[3] W. Lohmann, R. Kopp and R. Voss, CERN 85-03, Geneva (1985).
[4] W. Lohmann, R. Kopp and R. Voss, MUDEX – Program Description, CERN, private communication.
[5] H.J. Bhabha, Proc. Roy. Soc. A164 (1938) 257.
[6] A.A. Petrukhin and V.V. Shestakov, Can J. Phys. 46 (1968) S377.
[7] R.P. Kokoulin and A.A. Petrukhin, Acta Phys. Hung. 29 suppl. 4 (1970) 277; Proc. 12th Int. Conf. on Cosmic Rays, Hobart (1971) vol. 6, p. A2436.
[8] B. Anders et al., ZEUS Collab., DESY-Report 86-105, Hamburg (1986).
[9] W.R. Nelson, H. Hirayama and D.W.O. Rogers, SLAC-Report-265 (1985).
[10] U. Behrens, private communication.
[11] H. Brückmann, Proc. Workshop on compensated Calorimetry, Pasadena, CALT-68-1305 (1985).
[12] H. Brückmann, U. Behrens and B. Anders, Nucl. Instr. and Meth. A263 (1988) 136, and DESY 86-155, Hamburg (1986).
[13] E. Bernardi, internal DESY-Report F1-87-01.
[14] J.E. Moyal, Phil. Mag. 46 (1955) 263.
[15] H. Hirayama, S. Ban and S. Miura, KEK Preprint 86-97, Japan (1987) submitted to Nucl. Sci. Eng.
[16] R. Wigmans, CERN/EP 86-141, Geneva (1986).
[17] E. Bernardi et al., ZEUS Collab., DESY-Report 87-041, FTUAM-EP-87-03, Hamburg (1987).